Linear Optics Verification for PEP-II using Model-Independent Analysis *

Y.T. Yan, Y. Cai, J. Irwin, and M. Sullivan, SLAC, Stanford, CA 94309, U.S.A.

Abstract

We verify all quadrupole strengths (both normal and skew) and determine sextupole feed-downs as well as all BPM gains and BPM cross-plane couplings by an SVD-enhanced least-squares fitting of the phase advances (only those which are accurately determined) and the Green's functions (specified by the local transfer matrix components R12, R34, R32, and R14). The phase advances and the Green's functions are obtained by analyzing turn-by-turn Beam Position Monitor (BPM) data from high-resolution model-independent analysis (MIA). Once the magnet strengths are verified, a magnet correction priority sequence can be exercised in the computer before one tries to correct the real accelerator. Results from PEP-II LER measurement are presented.

1 INTRODUCTION

Local Green's functions between BPMs derived from orbit measurement have been considered for comparing an accelerator machine optics with those calculated from the lattice model [1] using model-independent analysis (MIA) [2]. In this paper, along with the local green functions we include phase advances (which usually can be determined accurately) between BPMs to improve the least-squares fitting accuracy.

Taking the PEP-II Low-Energy Ring (LER) as an example, we describe the BPM buffer data acquisition in section 2, and the extraction of 4 independent linear orbits in section 3. In section 4, we describe how phase advance between BPMs is calculated and used for fitting. In section 5, we review the computation of the local linear Green's functions specified by values of the transfer matrix components, $\mathcal{R}_{12}, \mathcal{R}_{14}, \mathcal{R}_{32}$, and $\mathcal{R}_{34}$. In section 6, we briefly describe how we carry through an iterative process for the SVD-enhanced least-squares fitting. In section 7, we present typical results from an application to the PEP-II LER.

2 BPM BUFFER DATA ACQUISITION

In the PEP-II LER, currently there are 319 BPMs of which 152 BPMS are single-view horizontal (X) BPMs, 142 BPMs are single-view vertical (Y) BPMs, and 25 BPMs are double-view (X,Y) BPMs. Therefore, one-turn BPM buffer data can offer a maximum of 177 X data and 167 Y data. Unlike linacs where there is often enough incoming jitter in the beam to measure and identify betatron modes, in the rings, to offset radiation damping, the beam is resonantly excited by a shaker at the horizontal betatron (eigen) tune and then at the vertical betatron (eigen) tune, each for 2800 turns to get a complete set of data which are stored in 2 sets of matrices, one set for the horizontal and the other set for the vertical excitation. Each set has two matrices, one 2800-by-177 matrix for storing x data and one 2800-by-167 matrix for storing y data. There may be bad BPMs and so the columns are reduced accordingly.

3 EXTRACTION OF INDEPENDENT LINEAR ORBITS

Upon performing an FFT on each column of the data in the matrices, besides the 0-th FFT mode representing the self-consistent closed orbit, one finds a dominant FFT mode at the resonance excitation eigen frequency, representing the two degrees of freedom of the betatron motion for each excitation. The cosine-like orbit is represented by the real part and the sine-like orbit is represented by the imaginary part. Therefore, a total of 4 independent linear (X and Y) orbits can be extracted from the two eigen-mode excitations. Shown in figure 4 are typical independent linear orbits. One can clearly see the coupling in these orbits.
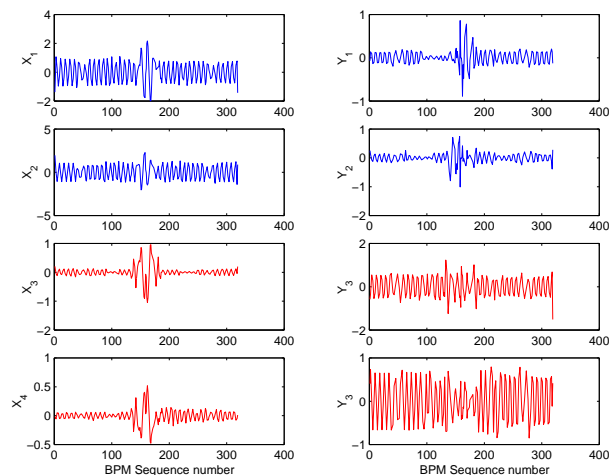

Figure 1: Four independent orbits extracted from PEP-II LER BPM buffer data. The first two orbits (x1, y1) and (x2, y2) are extracted from beam orbit excitation at the horizontal tune while the other two orbits (x3, y3) and (x4, y4) are from excitation at the vertical tune.

4 PHASE ADVANCES

If there is no BPM cross coupling, one can calculate the orbit betatron phase at each BPM location by simply taking the arctangent of the ratio of the imaginary part to the real part of the resonance excitation FFT mode. Phase advances between adjacent BPMs can then be calculated by subtraction. Note that these phase advances are independent of the BPM gains because they are cancelled in the ratio. BPMs with cross-coupling errors are excluded from phase advance fitting. They can be found during the fitting process and based on previous experience. The fitting process allows for non-zero BPM cross coupling. If any BPM cross coupling becomes larger than a small cut-off, then the phase advance condition at the BPM is dropped.

5 LINEAR GREEN'S FUNCTIONS

Though x' and y' are not directly measured they exist. Given the above complete set of 4 independent orbits obtained from one horizontal excitation and one vertical excitation, one can conceptually form a non-singular matrix at the ath or the bth BPM consisting of the phase-space coordinates: eg.

$$Z^a = \begin{pmatrix} x_1^a & x_2^a & x_3^a & x_4^a \\ x_1'^a & x_2'^a & x_3'^a & x_4'^a \\ y_1^a & y_2^a & y_3^a & y_4^a \\ y_1'^a & y_2'^a & y_3'^a & y_4'^a \end{pmatrix} .$$

Applying the symplectic condition (damping is offset by the excitation to an equilibrium state), one obtains the invariants (constants around the ring) represented by an antisymmetric matrix $Q = Z^{b\,T} J Z^b = Z^{a\,T} J Z^a$. This antisymmetric invariant matrix contains, in general, 6 scalar invariants. However, since the shaker is excited at the two eigen tunes, it can be shown that only the two non-coupled invariants Q_{12}, Q_{34} are not 0; $Q_{13} = Q_{14} = Q_{23} = Q_{24} = 0$. Applying the symplectic property of the transfer map, $\mathcal{R}^{ab\,T} J \mathcal{R}^{ab} = J$, and relationship between phase-space coordinates and measured orbits, (x_1, y_1), (x_2, y_2), (x_3, y_3), (x_4, y_4) to the linear phase-space coordinates transfer relationship between a and b given by $Z^b = \mathcal{R}^{ab} Z^a$, one obtains the following 4 equations [1]:

$$(x_1^a x_2^b - x_2^a x_1^b)/Q_{12} + (x_3^a x_4^b - x_4^a x_3^b)/Q_{34} = \mathcal{R}_{12}^{ab} . \quad (1)$$

$$(x_1^a y_2^b - x_2^a y_1^b)/Q_{12} + (x_3^a y_4^b - x_4^a y_3^b)/Q_{34} = \mathcal{R}_{32}^{ab} . \quad (2)$$

$$(y_1^a x_2^b - y_2^a x_1^b)/Q_{12} + (y_3^a x_4^b - y_4^a x_3^b)/Q_{34} = \mathcal{R}_{14}^{ab} . \quad (3)$$

$$(y_1^a y_2^b - y_2^a y_1^b)/Q_{12} + (y_3^a y_4^b - y_4^a y_3^b)/Q_{34} = \mathcal{R}_{34}^{ab} . \quad (4)$$

The RHS's are always Green's function elements, $\mathcal{R}_{12}, \mathcal{R}_{32}, \mathcal{R}_{14}, \mathcal{R}_{34}$; the first index is 1 or 3 according to whether 'b' is horizontal or vertical, and the second index is 2 or 4 according to whether 'a' is horizontal or vertical. One or two or four of the above equations will apply depending on whether the two BPMs at 'a' and 'b' are both single-view or only one single-view or both double-view BPMs. Note that the amplitude and orthogonality of the 4 modes being used enters through Q_{12} and Q_{34}.

These linear Green's functions for all combinations of (a,b) are not completely independent from each other. Since there are 4 measurements at each single-view BPM, 1 for each of the 4 orbits, one might expect each BPM to be involved in 4 independent equations (assuming no BPM gain errors). This is indeed true: there are 2 independent "normal" measurements and 2 independent "skew" measurements. For double-view BPMs one expects eight relationships. One can show that all Green's function elements may be expressed in terms of elements between neighbors and next-nearest neighbors.

In order to include the BPM errors into the least-squares fitting process, the Green's functions in the BPM measurement frame, as given by Eqs. 1-4, are expressed as follows.

$$\mathcal{R}_{12}^{ab} = g_x^b R_{12}^{ab} g_x^a + g_x^b R_{14}^{ab} \theta_{xy}^a + \theta_{xy}^b R_{32}^{ab} g_x^a + \theta_{xy}^b R_{34}^{ab} \theta_{xy}^a,$$

$$\mathcal{R}_{32}^{ab} = g_y^b R_{32}^{ab} g_x^a + g_y^b R_{34}^{ab} \theta_{xy}^a + \theta_{yx}^b R_{12}^{ab} g_x^a + \theta_{yx}^b R_{14}^{ab} \theta_{xy}^a,$$

$$\mathcal{R}_{14}^{ab} = g_x^b R_{14}^{ab} g_y^a + g_x^b R_{12^{ab}} \theta_{yx}^a + \theta_{xy}^b R_{34}^{ab} g_y^a + \theta_{xy}^b R_{32}^{ab} \theta_{yx}^a,$$

$$\mathcal{R}_{34}^{ab} = g_y^b R_{34}^{ab} g_y^a + g_y^b R_{32}^{ab} \theta_{yx}^a + \theta_{yx}^b R_{14}^{ab} g_y^a + \theta_{yx}^b R_{12}^{ab} \theta_{ya}^a,$$

where g_x's, g_y's are the BPM gains, and θ_{xy}'s and θ_{yx}'s are the BPM cross-coupling multipliers. $R_{12}, R_{34}, R_{32}, R_{14}$ are the Green's functions of the machine.

6 SVD-ENHANCED LEAST-SQUARES FITTING

Using the expression for local linear Green's functions and the phase advances between BPMs, we can start an SVD-enhanced least-squares fitting by initializing BPM gains and cross couplings and the quadrupole and sextupole feed-down variables in the lattice model with a reasonable guess (for example, initialization with the machine configuration). To ease the programmatic fitting process, we form all variables and all measurement derived quantities (phase advances and the independent Green's functions) into one-dimensional arrays, i.e. vectors, represented by $\vec{X}$ and $\vec{Y}m$ respectively. The corresponding parameters from the model, which are implicit functions of all the fitting variables, are also formed into a vector functional form given by $\vec{Y}(\vec{X})$. Denoting the reasonably guessed variable values as $\vec{x}_o$, and letting $\vec{X} = \vec{x}_o + \vec{x}$, one has

$$\vec{Y}(\vec{x}_o + \vec{x}) = \vec{Y}(\vec{x}_o) + M\vec{x} + \vec{\eta}(\vec{x}) = \vec{Y}m,$$

where $\vec{\eta}(\vec{x})$ contains nonlinear terms of the the Taylor expansion of $\vec{Y}(\vec{x}_o + \vec{x})$, which is ignored in the iteration equation given by

$$M\vec{x} = \vec{Y}m - \vec{Y}(\vec{x}_o) = \vec{b}.$$

Since there could be degeneracies causing the least-squares fitting solution, $\vec{x} = (M^T M)^{-1} M^T \vec{b}$, to diverge, we use an SVD-enhanced least-squares fitting which solves the above iteration equation by selecting dominant SVD modes. At each iteration, the guessed variable values, $\vec{x}_o$ is updated and so the linear derivative matrix, M, is also updated for the next iteration.

Through iterations, the corresponding phase advances and local linear Green's functions calculated from the model get much closer to those measured. Once the residuals can no longer be reduced, the iterative process stops.
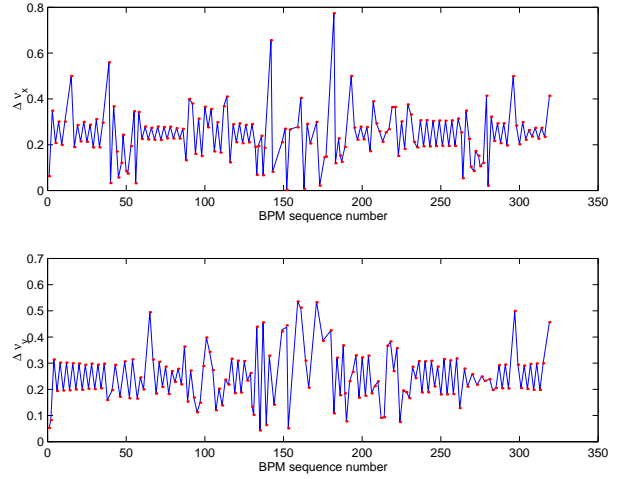

Figure 2: Comparison of the phase advances from measurement and model for the horizontal eigen plane (top) and the vertical eigen plane (bottom). The lines show the phase advances measured between BPMs while the dots show the corresponding phase advances calculated from the ideal lattice model before least-squares fitting. (BPM buffer data acquired on April 9, 2002 from the PEP-II LER.)

7 RESULTS FROM APPLICATION TO THE PEP-II LER

We have applied the above SVD-enhanced least-squares Fitting procedure to the PEP-II LER. Comparison of the phase advances derived from the orbits and model are shown in Figure 2 before fitting and Figure 3 after fitting. Comparison of the Green's functions (R12 and R34) from measurement and model are shown in Figure 4 before fitting and Figure 5 after fitting for a typical case. Once the fitting procedure has converged the machine is linearly verified.

Once the linear machine lattice is verified, one-turn matrices at all magnet, marker, and BPM locations can be calculated. The beta functions, linear coupling angles, and linear coupling strengths can then be derived from these one-turn matrices. Figure 6 compares the verified beta functions with that of the idea lattice model at BPM locations while figure 7 shows beta functions in the vicinity of IP where the verified β_x^* and β_y^* are also shown. At each interested location, the verified beta functions are obtained from the

Figure 3: Comparison of the phase advances from measurement and fitted model for the horizontal eigen plane (top) and the vertical eigen plane (bottom). The lines show the phase advances measured between BPMs while the dots show the corresponding phase advances calculated from the lattice model after SVD-enhanced least-squares fitting. (BPM buffer data acquired on April 9, 2002 from the PEP-II LER.)

one-turn linear maps extracted from the fitted model, that is, from the verified machine lattice.
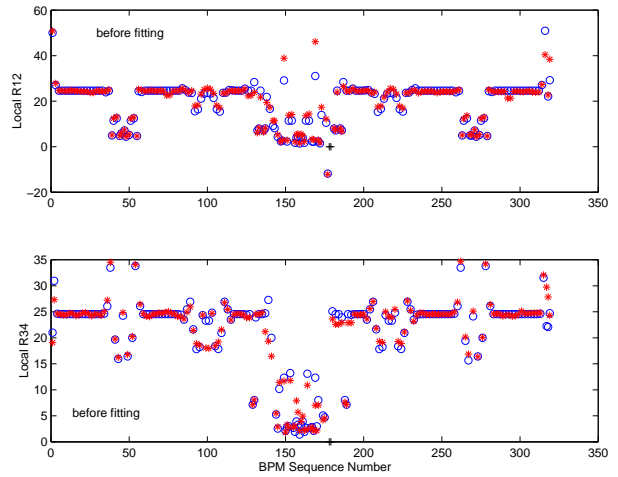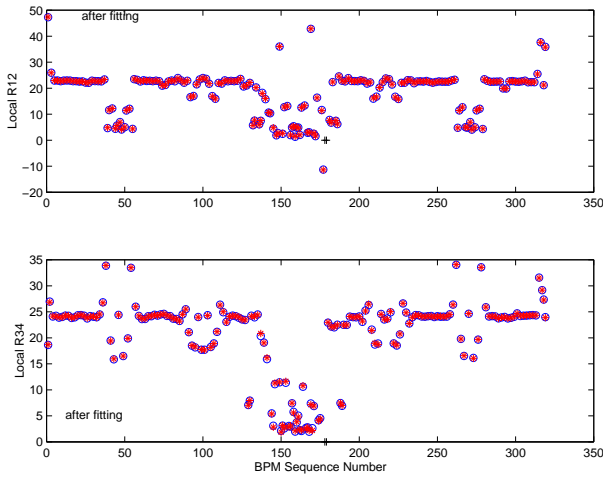

Figure 4: Comparison of local Greens' functions, $\mathcal{R}_{12}$ and $\mathcal{R}_{34}$, between measurement and that calculated from lattice model before fitting. The stars are from measurement while the circles are from the lattice model. (BPM buffer data acquired on April 9, 2002 from the PEP-II LER.)

The verified machine lattice can guide the real machine corrections. For example, Figure 6 shows beta beating for the verified machine on April 9, 2002 (also shown in Figure 8 for a re-scaled plot). Indeed, there was significant beta beating for the PEP-II LER. Although this beating has no negative effect on the PEP-II performance at the working tunes as can be shown in Figure 7, the verified beta functions (β^*'s) are favorably smaller than those

Figure 5: Comparison of local Greens' functions, $\mathcal{R}_{12}$ and $\mathcal{R}_{34}$, between measurement and that calculated from lattice model after fitting. The fitting variables are all BPM gains and cross-plane couplings and the strengths of the quad families and quad skews and sextupole feed-downs. The stars are from measurement while the circles are from the lattice model. (BPM buffer data acquired on April 9, 2002 from the PEP-II LER.)
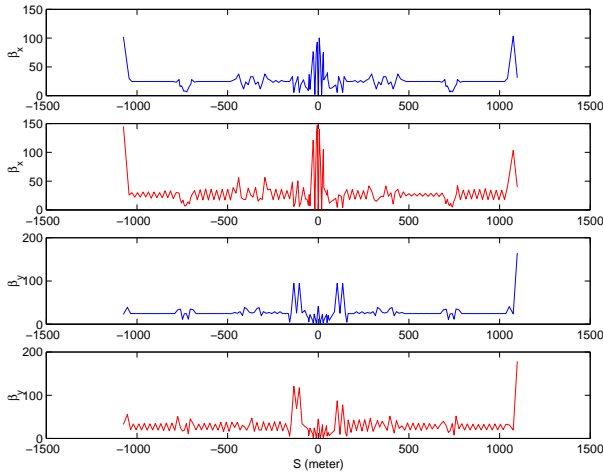

Figure 6: Comparison of the verified beta functions with those of the idea lattice model at BPM locations. (a) horizontal beta functions for ideal lattice model; (b) verified horizontal beta functions; (c) vertical beta functions for ideal lattice model; (d) verified vertical beta functions; (BPM buffer data acquired on April 9, 2002 from the PEP-II LER.)

of the ideal lattice. The beating resulting from coupling may be one of the major reasons for the trouble in adjusting the horizontal working tune closer to a half integer in order to reduce the beam-beam effects. The effect of reducing a skew quad (SK4) to 45% of its verified strength of 4.1 Tesla is shown in Figure 9 which displays reduced beta beating and in Figure 10 which displays reduced variation of the phase advances in the arcs as compared to Figure 3.
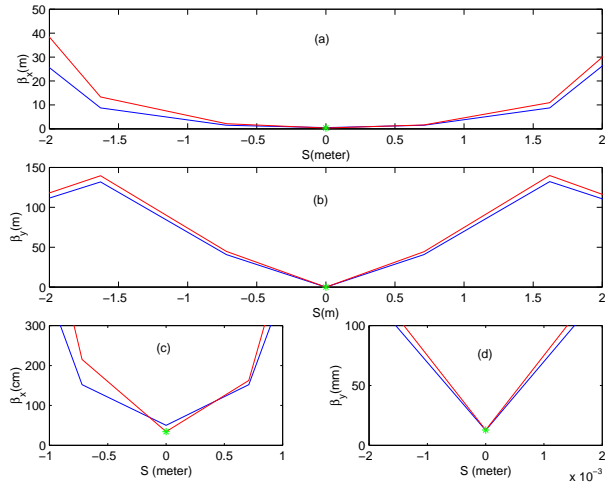

Figure 7: Comparison of the beta functions in the vicinity of IP for the horizontal beta functions (a and c) and the vertical beta functions (b and d). The blue lines are for those calculated from the ideal lattice model while those calculated from the verified machine lattice are represented by the red lines (bottom at IP where S=0, but top on both sides of the plot) Note that β_y^* is close to the designed value as shown in (d) while the β_x^* is smaller than the designed value as shown in (c). (BPM buffer data acquired on April 9, 2002 from the PEP-II LER.)

This reduced beta beating is also verified in the most recent data acquired on June 13, 2002 from the PEP-II LER (with a reduced SK4) as shown in Figure 11, displaying reduced variation of the measured phase advances in the arcs as compared to Figure 3.
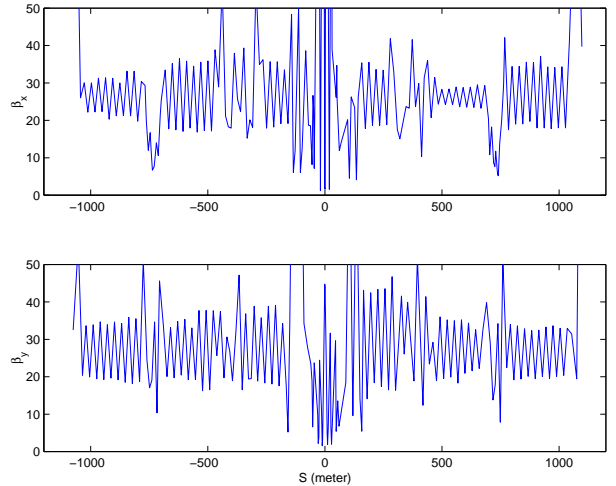

Figure 8: The verified beta functions with a smaller vertical scale in the plots to show beta beatings. Note that at the arcs, the ideal beta functions should have the same values. (BPM buffer data acquired on April 9, 2002 from the PEP-II LER.)
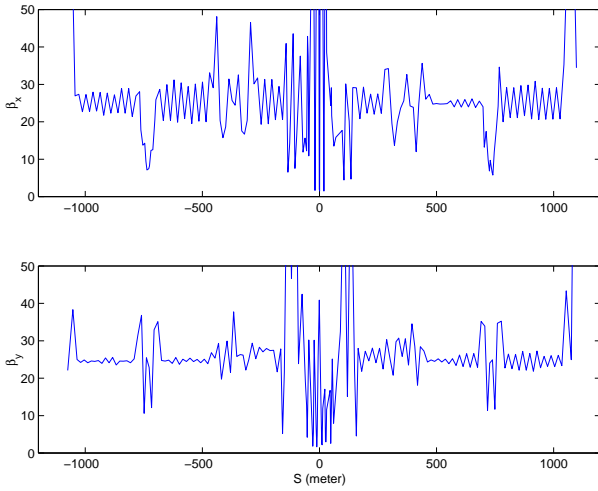
Figure 9: The beta functions with a reduced skew (SK4) value that shows much reduced beta beatings. Note that at the arcs, the ideal beta functions should have the same values. (BPM buffer data acquired on April 9, 2002 from the PEP-II LER.)
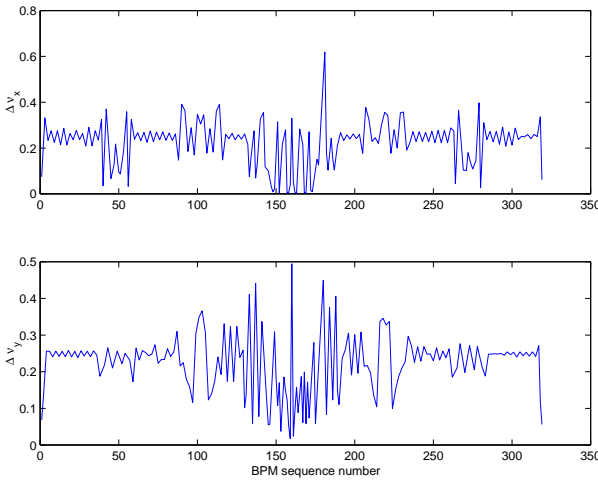

Figure 10: The phase advances with a reduced skew (SK4) value that shows reduced beta beatings. Note that at the arcs, the ideal phase advances should have the same values. (BPM buffer data acquired on April 9, 2002 from the PEP-II LER.)
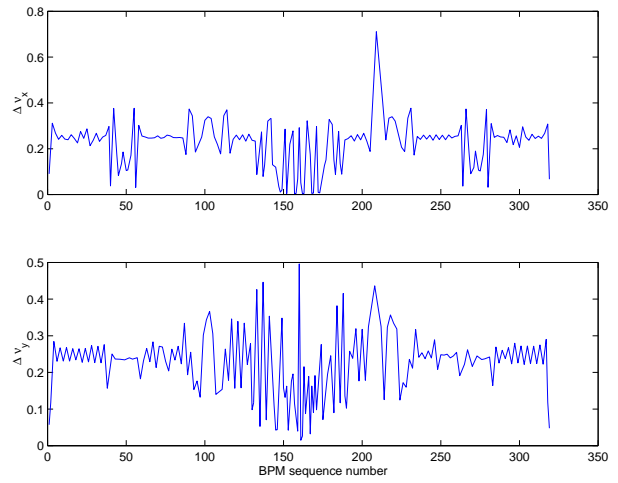

Figure 11: The measured phase advances with a reduced skew (SK4) value that shows reduced beta beatings. Note that at the arcs, the ideal phase advances should have the same values. Also note that the large phase advances (ν_x) at BPM number 209 is due to missed BPM number 208 which is excluded because of bad data. (BPM buffer data acquired on June 13, 2002 from the PEP-II LER.)

9   ACKNOWLEDGEMENT

10   REFERENCES

[1] J. Irwin, and Y.T. Yan, "Beamline model verification using model-independent analysis" SLAC-PUB-8515 (2000), in EPAC2000 Conference Proceedings; Y. Cai, J. Irwin, M. Sullivan, and Y.T. Yan, in PAC2001 Conference Proceedings.

[2] J. Irwin, C.X. Wang, Y.T. Yan, et. al., "Model-Independent Beam Dynamics Analysis," Phys. Rev. Lett. **82**, 1684 (1999).

8   SUMMARY

With SVD-enhanced least-squares fitting, we fit the local Green's functions and phase advances between measurement and lattice model. The fitting results can identify malfunctioning BPMs and magnet strength differences between the machine and the lattice model. Once the magnet strengths are verified. we can exercise an accelerator optics correction in the computer with the verified machine lattice before actually correcting the machine.